Parity-odd Neutrino Torque Detection

Hao-Ran Yu,[1,2,3,*] Ue-Li Pen,[2,1,4,5,6,†] and Xin Wang[2,‡]

[1] *Tsung-Dao Lee Institute, Shanghai Jiao Tong University, Shanghai, 200240, China*
[2] *Canadian Institute for Theoretical Astrophysics, University of Toronto, M5S 3H8, Ontario, Canada*
[3] *Department of Astronomy, Shanghai Jiao Tong University, Shanghai, 200240, China*
[4] *Dunlap Institute for Astronomy and Astrophysics, University of Toronto, Toronto, ON M5S 3H4, Canada*
[5] *Canadian Institute for Advanced Research, CIFAR Program in Gravitation and Cosmology, Toronto, ON M5G 1Z8, Canada*
[6] *Perimeter Institute for Theoretical Physics, Waterloo, ON N2L 2Y5, Canada*

(Dated: October 24, 2018)

Cosmological observations are promising ways to improve of our understandings of the neutrino mass properties. The upper bound on their sum of mass is given by the cosmic microwave background and large scale structures. These measurements are all parity-even. Here we show that, the presence of neutrino mass provides a unique contribution to the directions of the angular momentum of galaxies, which is the first parity-odd neutrino effect on large scale structures. This parity-odd observable is free of the contamination of the linear perturbation theory, and can be cleanly separated from other non-gravitational effects. A complete 21-cm neutral Hydrogen halo survey deep to redshift 1 can give a 5σ confidence level of detecting the neutrino torque effect if the sum of neutrino masses is 0.05 eV.

Introduction.— Neutrino mass is a long-standing physics problem. The flavour oscillation experiments [1] discovered the mass splittings of neutrinos and placed a lower bound of the sum of their mass $M_\nu \equiv \sum_{i=1}^{3} m_{\nu_i} \gtrsim 0.05$ eV [2]. The existence of neutrino mass has profound impacts on cosmic evolution. In the early Universe relativistic neutrinos modulate the matter-to-radiation ratio, and based on which the cosmic microwave background observations provide an upper bound of $M_\nu \lesssim 0.23$ eV [3]. In the late Universe, neutrinos become non-relativistic, and contribute to the matter energy density Ω_m. Unlike the majority of matter, the cold dark matter (CDM) and baryons, neutrinos maintain a high velocity dispersion, known as "free streaming", which reduces their gravitational collapse on small scales. A number of large scale structure (LSS) surveys (such as Euclid [4], LSST [5], eBOSS [6], WFIRST[7], and DESI [8]) are aimed to improve this upper bound using neutrino effects on LSS, however we usually encounter difficulties in disentangling neutrino effects from other parameters, and in understanding halo bias and cosmic variance. Recently, new nonlinear neutrinos effects on LSS are proposed to give independent measurements on neutrino mass [9–11]. For these effects one needs to carefully separate and exclude the contaminations from non-gravitational contributions. The only clean, gravitational-only neutrino effect on LSS is the damping of weak gravitational lensing power spectrum [3]. However the amount of information and constraining power of the lensing is limited by the projection onto the 2-dimensional sky. Is there a 3-dimensional measure which is cleanly gravity-driven, to measure the neutrino mass?

The angular momentum. The angular momenta (spin) of dark matter halos or galaxies originated by clean gravitational interactions. Unlike parity-even tidal and density fields, the linear perturbation theory (other effects and bias) cannot contaminate a parity-odd spin measurement. Here we present the neutrino torque effect, to modulate the spin of dark matter halos.

Theory.— In the picture of LSS formation, gravitational instability lets initial density fluctuations form dark matter halos, in which galaxies are embedded. In these highly nonlinear structures, uncertainties of halo bias, halo merging history and baryonic mechanisms obstruct us from clearly understanding the statistics like number counts and morphologies. In comparison, the spins of galaxies/halos represent a local probe of gravity, especially contributed from the linear epoch of the structure formation.

In the tidal torque theory, the spin of a halo in Lagrangian space $\boldsymbol{j}_L \propto \int_{V_L} \boldsymbol{q} \times \boldsymbol{\nabla}\phi \mathrm{d}^3\boldsymbol{q}$ can be written in first order as $\boldsymbol{j}_I \propto \boldsymbol{\epsilon}\mathbf{I}\mathbf{T}$ [12], where ϕ is the gravitational potential, $\boldsymbol{q}$ is the Lagrangian coordinates relative to the center of mass of the protohalo in volume V_L, $\mathbf{I}_q = (I_{ij}) = (\int_{V_L} q_i q_j \mathrm{d}^3\boldsymbol{q})$ is the protogalactic inertia tensor, $\mathbf{T} = (T_{ij}) = (\partial_i\partial_j\phi)$ is the local tidal shear tensor, and $\boldsymbol{\epsilon} = (\epsilon_{ijk})$ is the Levi-Civita symbol to collect the asymmetric components generated by the misalignment between $\mathbf{I}_q$ and $\mathbf{T}$. This spin grows at first order in the early Universe [12]. Actually, as halos collapse, nonlinear gravity field is hard to torque small objects, and the spin directions are expected to be contributed mostly in the linear regime. These concepts can be straightforwardly tested in numerical simulations. In Lagrangian space, CDM and baryonic matter are torqued by the same gravitational shear, so the spin direction is not affected by baryonic effects. If a halo has a merging history, it sim-

* haoran@cita.utoronto.ca
† pen@cita.utoronto.ca
‡ xwang@cita.utoronto.ca

ply collects disconnected regions in Lagrangian space but conserves their total spin.

Massive neutrinos contribute sub-percent fraction of the matter ingredient, and their unique spatial distribution and evolution should contribute a unique torque to halos and galaxies. In particular, neutrino density field traces CDM on large scales while their small scale structures are smoothed out by their high velocity dispersion, known as the free-streaming. They contribute a predictable tidal tensor $\mathbf{T}_\nu(m_{\nu_i})$ depending on the their mass. The interplay between $\mathbf{I}_q$ and $\mathbf{T}_\nu$ leads to an additional neutrino torque $\boldsymbol{j}^I_\nu \propto \boldsymbol{\epsilon}\,\mathbf{I}_q\,\mathbf{T}_\nu$. Integrated neutrino torque over cosmic evolution, we get the neutrino modulation of the halo spin,

$$\boldsymbol{j}^I_{\nu 0} = \int a(\tau)D(\tau)\boldsymbol{\epsilon}\mathbf{I}(\tau)\mathbf{T}_\nu(\tau)\mathrm{d}\tau. \qquad (1)$$

Here, τ is the Newtonian time, $D(\tau)$ is the growth factor, and other quantities are functions of time.

Reconstruction.— The feasibility of prediction of the neutrino tidal torque relies on the precision reconstruction of the cosmic evolution history. There are many emerging reconstruction methods. For example, the isobaric halo reconstruction can recover the initial conditions of the universe from spatial distribution of halos. In the case of high number densities the reconstructed density field is correlated with the true initial density field on scales $k \lesssim 0.7h$/Mpc [13], close to the limit ($k \lesssim 1h$/Mpc) of isobaric reconstruction from using direct CDM density field [14], or the limit of reconstruction from the true displacement field [15]. ELUCID simulation are able to reconstruct the local Universe [16]. These reconstruction techniques enable us to study the tidal field from both CDM and neutrinos in an unprecedented precision, at different epochs of the cosmic evolution. Neutrinos share the same Fourier phases of CDM, reconstructed from halo reconstruction, but only differ by the ratio of their linear transfer function, depending on the neutrino masses. The final neutrino torque can be understood as the interaction between large (neutrino free streaming) and small (collapsing) scales.

To apply Eq.(1), $\mathbf{I}_q$ is also required to be reconstructed. Firstly, we note the fact that, during the initial conditions, the $\mathbf{I}_q$ and $\mathbf{T}_c$ are highly correlated in Lagrangian space [17, 18], which can be understood that $\mathbf{I}_q$ is a collection of matter to be shell-crossed to form a halo, being parallel with $\mathbf{T}_c$. Secondly, in the linear, intermediate epochs, $\mathbf{I}_q$ is firstly reshaped according to the dominating $\mathbf{T}_c$, thus the linear evolved $\mathbf{T}_\nu(\tau)$ will act on an evolved $\mathbf{I}(\tau)$. Further, $\mathbf{I}(\tau)$ will be affected by nonlinear effects, which are more difficult to predict, however halos are relatively small and their spin directions can hardly be changed dramatically. A deeply study of the second step above is beyond the scope of this letter. Here we show that, even simplified to the first point above, the total neutrino torque can still be reconstructed.

We construct an equivalent inertia $\mathbf{I}_r$ from $\mathbf{T}_c$, in order that $\boldsymbol{\epsilon}\,\mathbf{I}_r\mathbf{T}_\nu$ is maximumly correlated with $\boldsymbol{j}^I_{\nu 0}$ from

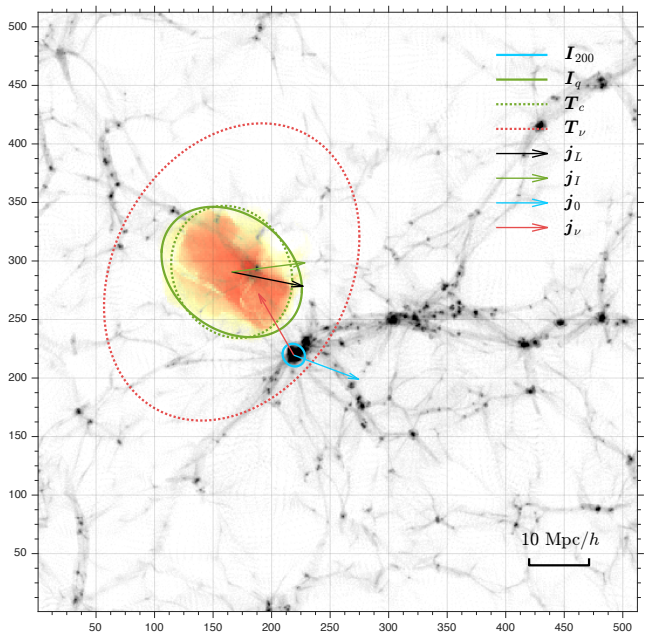

FIG. 1. Visualization of the neutrino torque. We show the LSS slice centered at a selected halo with depth twice the halo radius r_{200}. Equivalent ellipsoids by solid lines show the moment of inertia in Lagrangian and Eulerian space $\mathbf{I}_q$ and $\mathbf{I}_{200}$, while dotted ellipsoids show the tidal shear from CDM and neutrinos $\mathbf{T}_c$ and $\mathbf{T}_\nu$. $\boldsymbol{j}_L$, $\boldsymbol{j}_0$ are the Lagrangian and Eulerian halo spins, whereas $\boldsymbol{j}_I$ is the tidal torque prediction. The initial neutrino torque is shown by $\boldsymbol{j}_\nu$.

Eq.(1). In the primary coordinate of $\mathbf{T}_c$, $\mathbf{T}_c$ can be eigen-decomposed as $\mathbf{T}_c = \sum_{i=1}^3 \mathbf{T}_c^{\lambda_i}$ and find α_i such that the reconstructed

$$\mathbf{I}_r = \sum_{i=1}^{3} \alpha_i \mathbf{T}_c^{\lambda_i} \qquad (2)$$

optimizes the cross-correlation $\mu(\boldsymbol{j}^I_{\nu 0}, \boldsymbol{j}^{I_r})$, where

$$\boldsymbol{j}^{I_r}_\nu = \boldsymbol{\epsilon}\,\mathbf{I}_r\mathbf{T}_\nu \qquad (3)$$

is the reconstructed neutrino spin direction.

Simulation.— These correlations and coefficients are tested across a set of high-resolution N-body simulations [19]. Given any halo formed in the simulation, all the belonging particles are mapped back to Lagrangian space. The status of this definite set of particles can be traced in a resimulation of the exact same initial conditions.

In Fig.1 (all quantities are projected onto the plane of this letter), we select a very massive halo ($7.8 \times 10^{14} M_\odot$) to maximize the clarity of the visualization of the halo properties. Note that these properties (cross-correlations) have only weak dependence on halo mass. The background LSS at redshift $z = 0$ has the thickness $2r_{200}$ with r_{200} being the halo radius within which the mean halo density is 200 times the mean matter density of the Universe. The Lagrangian mapping of this

halo is shown by the protohalo's column density with the orange clouds. To visualize the tidal torque theory, we plot ellipsoids equivalent to $\mathbf{I}_q$ and $\mathbf{I}_{200}$, where $\mathbf{I}_{200}$ is the moment of inertia within r_{200}. The ellipsoids with dotted lines correspond to $\mathbf{T}_c$ and $\mathbf{T}_\nu$, normalized such that their volumes are V_L and $8V_L$ respectively. As expected, $\mathbf{I}_q$ and $\mathbf{T}_c$ are aligned with their primary axes in parallel with the collapsing direction, or perpendicular to the filament below. Their minor misalignment yields the tidal torque $\boldsymbol{j}_I$ (all the spin arrows are normalized to have 15 Mpc/h), which is the first order approximation of the true initial spin $\boldsymbol{j}_L$. They are, in general, highly correlated with the spin of the final halo $\boldsymbol{j}_0$. In comparison, the neutrino tidal shear $\mathbf{T}_\nu$ torques $\mathbf{I}_q$ in an other less correlated direction $\boldsymbol{j}_\nu$.

The validity of the tidal torque formulation is tested by an ensemble average over all halos, across 3 orders of magnitude in mass range, and over simulations with different resolutions. the cross-correlation coefficients $\langle \boldsymbol{j}(z)\cdot\boldsymbol{j}_L\rangle$ and $\langle \boldsymbol{j}(z)\cdot\boldsymbol{j}_I\rangle$ smoothly decrease from 1 to 0.80, and from 0.75 to 0.69, respectively.

For neutrinos, the first-order tidal torque approximation gives a perfect (with cross-correlation 0.99) representation of the actual neutrino torque and it has generally less than 0.2 cross-correlation with CDM torques. This is expected in that $\mathbf{T}_c$ dominates locally (power spectrum index?) whereas $\mathbf{T}_\nu$ is contributed beyond the neutrino free-streaming scale (is this a 4-point function?). These two species, however, have a highly correlated contribution in structure formation. When we consider the forces that the two species exerted to the protohalo, $\boldsymbol{F}_{c/\nu} \propto \int_{V_L} \boldsymbol{\nabla}\phi_{c/\nu}\mathrm{d}^3\boldsymbol{q}$, the cross-correlation between two species is as high as 0.86 (power spectrum index?).

By Eq.(1) we estimate the magnitude of integrated neutrino torque $\langle|\boldsymbol{j}_{0\nu}|/|\boldsymbol{j}_0|\rangle \simeq 3\times10^{-4}$. In particular, the effect given by the smoother distribution for neutrinos relative to CDM accounts 0.03, while the neutrino fraction $f_\nu = 3.5\times10^{-3}$ (for $M_\nu = 0.05$ eV) and the backreaction from neutrinos to CDM $\sqrt{8}$ contribute the rest.

Measured from simulations, $(\alpha_1,\alpha_2,\alpha_3) = (-0.18, 0.18, 0.02)$ in Eq.(2) optimizes the cross-correlation $\left\langle \boldsymbol{j}^I_{\nu 0}\cdot\boldsymbol{j}^{I_r}_{\nu}\right\rangle = 0.19$. In this case we need 5×10^9 halos to have a 5σ detection (see Appendix A). If we improve the reconstruction of $\mathbf{I}_R$, the lower limit of required halos is 2×10^8.

Discussion.— Accuracy and mass dependency: we notice that the cross-correlation coefficients between $\boldsymbol{j}_0$ and initial values $\boldsymbol{j}_L$ and $\boldsymbol{j}_T$ are prominently higher than what was measured in [17]. We investigate that numerical errors that may affect the results. P3M (particle-particle particle-mesh) algorithms result in higher cross-correlation between initial and final spins, compared to PM (particle-mesh), where additional tangential forces in PM violate the angular momentum conservation. Higher mass halos in a given simulation generally have slightly higher μ_L and μ_I, however the correlation is enhanced greatly as we use higher mass resolutions. All other cross-correlation measurements have only weak dependencies on the halo mass, even in a fixed simulation. With different box sizes, mass resolutions, force resolutions, and find that the results are consistent across these simulations. Especially, in the estimation of number of halo spins needed to detect the neutrino torque, the deciding number is the cross-correlation $\left\langle \boldsymbol{j}^I_{\nu 0}\cdot\boldsymbol{j}^{I_r}_{\nu}\right\rangle = 0.19$. This has a very weak dependence on halo mass and configuration of the simulation.

Baryonic effects (+ etc.) in reconstruction and angular momentum conservation:

Observability: surveys like the Hubble Sphere Hydrogen Survey (HSHS) [20] can cover 1 billion galaxies. There are xxx HI galaxies with redshift 1 [21].

Beyond standard models: it was also suggested that neutrino mass is generated by a gravitational θ-term condensation as the source of dark energy [22].

Cosmic variance:

Bias:

cite later [23].

Conclusion.—

Acknowledgments.— We acknowledge funding from NSERC.

Appendix A: Errors in 3D

There are N halos with their unit spin vector randomly distributed on a 2D sphere, $|\boldsymbol{j}| = 1$ and $\langle\boldsymbol{j}\rangle = \mathbf{0}$. Adding an additional vector $a\hat{\boldsymbol{x}}$ ($a \ll 1$) to $\boldsymbol{j}$ and normalize we have $\boldsymbol{j}' = (\boldsymbol{j}+a\hat{\boldsymbol{x}})/|\boldsymbol{j}+a\hat{\boldsymbol{x}}|$, then we project $\boldsymbol{j}'$ onto $\hat{\boldsymbol{x}}$ and we get the signal $b = \boldsymbol{j}'\cdot\hat{\boldsymbol{x}}$. The numerical statistics are as following: $\langle b\rangle = 2a/3$ and $\sigma(b) = 1/\sqrt{3N}$. So, to get a $n\sigma$ detection,

$$N = 3n^2/4a^2 \tag{A1}$$

halos will be needed.

[1] Q. R. Ahmad *et al.*, Phys. Rev. Lett.**89**, 011301 (2002).
[2] K. A. Olive and Particle Data Group, Chinese Physics C **38**, 090001 (2014).
[3] P. A. R. Ade *et al.*, A&A**594**, A13 (2016).
[4] R. Laureijs *et al.*, ArXiv e-prints (2011), 1110.3193.
[5] LSST Science Collaboration *et al.*, ArXiv e-prints (2009), 0912.0201.
[6] K. S. Dawson *et al.*, Astron. J. **151**, 44 (2016).
[7] R. Goullioud *et al.*, Wide Field Infrared Survey Telescope [WFIRST]: telescope design and simulated perfor-

mance, in *Space Telescopes and Instrumentation 2012: Optical, Infrared, and Millimeter Wave*, volume 8442 of Proc. SPIE, p. 84421U, 2012.

[8] D. Eisenstein and DESI Collaboration, The Dark Energy Spectroscopic Instrument (DESI): Science from the DESI Survey, in *American Astronomical Society Meeting Abstracts*, volume 225 of *American Astronomical Society Meeting Abstracts*, p. 336.05, 2015.

[9] H.-M. Zhu, U.-L. Pen, X. Chen, D. Inman, and Y. Yu, Phys. Rev. Lett.**113**, 131301 (2014), 1311.3422.

[10] H.-M. Zhu, U.-L. Pen, X. Chen, and D. Inman, Phys. Rev. Lett.**116**, 141301 (2016), 1412.1660.

[11] H.-R. Yu *et al.*, Nature Astronomy **1**, 0143 (2017).

[12] S. D. M. White, ApJ**286**, 38 (1984).

[13] Y. Yu, H.-M. Zhu, and U.-L. Pen, ApJ**847**, 110 (2017).

[14] H.-M. Zhu, Y. Yu, U.-L. Pen, X. Chen, and H.-R. Yu, Phys. Rev. D**96**, 123502 (2017).

[15] H.-R. Yu, U.-L. Pen, and H.-M. Zhu, Phys. Rev. D**95**, 043501 (2017), 1610.07112.

[16] H. Wang, H. J. Mo, X. Yang, Y. P. Jing, and W. P. Lin, ApJ**794**, 94 (2014), 1407.3451.

[17] J. Lee and U.-L. Pen, ApJ**532**, L5 (2000), astro-ph/9911328.

[18] J. Lee and U.-L. Pen, ApJ**555**, 106 (2001), astro-ph/0008135.

[19] H.-R. Yu, U.-L. Pen, and X. Wang, The Astrophysical Journal Supplement Series **237**, 24 (2018).

[20] J. B. Peterson, K. Bandura, and U. L. Pen, ArXiv e-prints , astro (2006), astro-ph/0606104.

[21] M. A. Zwaan *et al.*, MNRAS**350**, 1210 (2004), astro-ph/0406380.

[22] G. Dvali and L. Funcke, Phys. Rev. D**93**, 113002 (2016).

[23] S. Codis *et al.*, MNRAS(2018), 1809.06212.